Stable helical peptoids *via* covalent side chain to side chain cyclization†

Belén Vaz and Luc Brunsveld*

Received 23rd April 2008, Accepted 4th June 2008
First published as an Advance Article on the web 26th June 2008
DOI: 10.1039/b806847j

Peptoids are oligomeric *N*-substituted glycines with potential as biologically relevant compounds. Helical peptoids provide an attractive fold for the generation of protein–protein interaction inhibitors. The generation of helical peptoid folds in organic and aqueous media has been limited to strict design rules, as peptoid-folding is mainly directed *via* the steric direction of α-chiral side-chains. Here a new methodology is presented to induce helical folds in peptoids with the aid of side chain to side chain cyclization. Cyclic peptoids were generated *via* solid-phase synthesis and their folding was studied. The cyclization induces significant helicity in peptoids in organic media, aids the folding in aqueous media, and requires the incorporation of only relatively few chiral aromatic side chains.

Introduction

Foldamers are oligomers that can adopt predictable secondary structures.[1] These secondary foldamer structures can be used as scaffolds mimicking naturally constrained secondary peptide structures, known to play a key role in protein–protein interactions, and modulate interactions between proteins.[2] In this field, peptoids, a specific class of foldamers, have emerged as candidates for pharmaceutical and chemical biology research.[3] Peptoids are oligomeric molecules based on *N*-substituted glycines which fold into specific conformations, depending on size, sequence and environment. Due to their oligomeric nature, peptoids can relatively easy be synthesized by standard solid-phase methods.[4] Additionally, peptoids are resistant to enzyme proteases.[5] These features make peptoids attractive bioactive oligomers to be applied for example for the modulation of proteins.[6] In contrast to other foldamers, such as β-peptides,[7] peptoids do not feature the possibility to form intramolecular backbone hydrogen bonds and lack stereochemistry in the backbone. Therefore, the intrinsic folding of peptoids in secondary structures is limited. Stable homochiral folds of peptoids are typically only obtained when the peptoid oligomer sequences follow strict steric and/or electronic requirements. The tendency to fold in well-ordered conformations is in those cases mainly directed by the steric constraints imposed by the side-chains and not by a structuring element in the backbone of the peptoid. Peptoids thus adopt homochiral helical secondary structures, especially when bulky side chains with a stereocenter close to the backbone are present.[8] Due to the steric interactions, the number of energetically accessible conformations of the peptoid is limited, resulting in oligomers of this type adopting a helical conformation with *cis* amide bonds, similar to the polyproline type I helix.[9]

Zuckermann *et al.* showed that in chiral helical peptoids all of the amide bonds of the major species were of *cis* geometry.[8,9] Although NMR experiments showed multiple species in slow exchange,[10] the major species was determined to be a regular helix with three residues per turn and a pitch of approximately 6 Å. Studies by Barron *et al.* showed the requirements for stable peptoid helices concerning chain length and sequence:[11] (1) *N*-α-stereocenters and aromatic substituents should be present in at least 50% of the monomer composition of the peptoid sequence, (2) in particular the last residue (at the *C*-terminus) should feature an α-chiral substituent and (3) the aromatic side-chain residues should be positioned to maximize inter side-chain aromatic π–π interactions, taking into account the repetitive disposition of three residues per turn. These design parameters result in relatively hydrophobic and long helical peptoid sequences, soluble and folding in organic solvents such as acetonitrile. The design parameters, however, typically do not support aqueous solubility. The number of peptoids folding into stable helical conformations in aqueous solution is therefore limited. Barron *et al.* have reported water-soluble amphiphatic peptoid helices featuring 12 residues or more, demonstrating high configurational stability, independent of solvent environment.[12] Shin and Kirshenbaum have prepared (*S*)-*N*-(1-carboxy-2-phenylethyl)glycine peptoid foldamers that are water soluble, due to the carboxyl functionality in the side chain.[13] The combination of the steric bulk in the side chain and the carboxyl functionalities allows for the folding of these peptoids in water, with control over their conformation by adjustment of the pH.

Typically, peptoids that fold into helical conformations in water are relatively long and feature many chiral aromatic side chains with little diversity. Aqueous solubility of these peptoids is mainly conferred by ionic side chains on one side of the helix. The hydrophobic aromatic groups are replaced with series of α-chiral hydrophilic side chains with amino, alcohol or carboxylic acid functional groups. In such a helical peptoid a 3-fold internal repetition pattern is adopted, allowing hydrophobic and hydrophilic residues to be methodically combined to create a peptoid with an amphiphilic surface, soluble in water.[12,14] Short helical peptoids are in general not accessible *via* this approach. Such smaller and diversely substituted helical peptoids are desirable for several

Max Planck Institute of Molecular Physiology, Otto-Hahn Straße 11, and Chemical Genomics Centre, Otto-Hahn Straße 15, D-44227, Dortmund, Germany. E-mail: luc.brunsveld@mpi-dortmund.mpg.de; Fax: +49 231 1332499; Tel: +49 231 97426473

† Electronic supplementary information (ESI) available: General information on peptoid purification and LC-MS and ESI-MS spectra of all peptoids (**1**–**22**). For ESI see DOI: 10.1039/b806847j

biological applications. Side chain to side chain cyclization has proven to provide a successful entry in stabilizing the helical fold of other types of oligomers in water[15] and has also found application in peptoid–peptide hybrids.[16] Head-to-tail cyclic peptoids have been shown to provide an entry to limit the number of accessible conformations.[17] Similarly, side chain to side chain cyclization *via* the Cu(I)-catalyzed [3 + 2] cycloaddition resulted in cyclic peptoids with a modified population of conformations in acetonitrile.[18]

Here we present the study of the effect of covalent side chain to side chain constraining elements on the stabilization of the helical fold of short peptoids, both in organic and aqueous media. A series of peptoids derived from the previously reported helical, but not water-soluble, 6*mer*- homopeptoid $(Nrpe)_6$, was designed, synthesized and studied. A covalent bridge between side chains of varying length was introduced at different positions in the oligomer. This resulted in cyclic peptoids featuring a lactam bridge at the relative positions *i* and *i* + 3 in the peptoid. Subsequently, water solubility conferring side-chains were inserted in the oligomer, replacing the (*R*)-*N*-(1-phenylethyl)glycine (Nrpe) functionalities, to investigate the helix stabilizing capacities of the side chain to side chain linkage in water.

Results and discussion

Peptoid design and synthesis

Three series of 6-*mer* peptoids were designed in order to investigate the effect of a lactam bridge between side chains of consecutive turns on the stabilization of the helical structure of the peptoids (Scheme 1). The homohexamer $(Nrpe)_6$[9] (Scheme 1) was synthesized and evaluated as a reference for the helical stability studies of the peptoids in organic solvents. Peptoid series 1 and 2 were designed to investigate the position and length of the constraining lactam bridge on helix stabilization in organic solvents. In the peptoid sequence two Nrpe functionalities were replaced by an aliphatic residue featuring a carboxylic acid and an aliphatic residue featuring an amine side chain functionality (Table 1). Linear analogs (**1–3** and **7–9**), with the possibility of forming a charge–charge interaction, and cyclic peptoids (**4–6** and **10–12**) were both designed to enable a comparison of the effects of a salt-bridge and a covalent bridge. A third series of peptoids was designed in which additional Nrpe functionalities were replaced by residues featuring polar side-chains. The overall content of residues with *N*-α-stereocenters and aromatic substituents was thus lowered to 50% or 33% and should allow the study of the folding in water. Similar as for series 1 and 2, series 3 featured

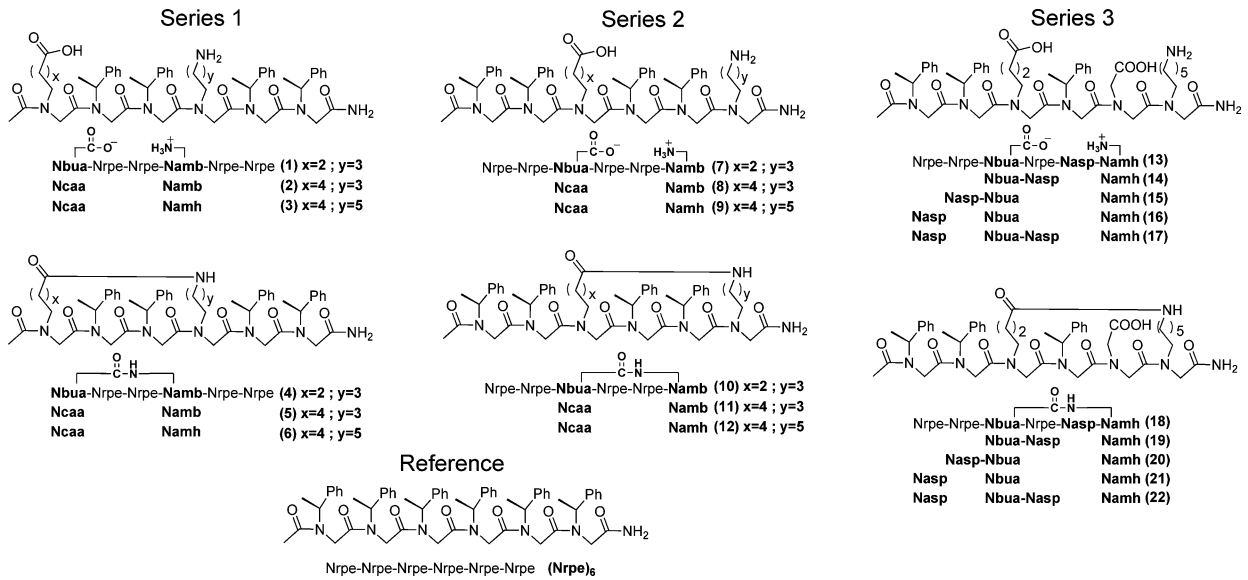

Scheme 1 Library of peptoids **1–22**, subdivided in series 1–3, and reference peptoid $(Nrpe)_6$. Nrpe = (*R*)-*N*-(1-phenylethyl)glycine, Ncaa = 6-aminocaproic acid, Nbua = 4-aminobutyric acid, Namh = 1,6-diaminohexane, Namb = 1,4-diaminobutane, Nasp = glycine.

Table 1 Amine building blocks for peptoids **1–22**

Structure	Resulting peptoid side chain
AllylOOC-$CH_2CH_2CH_2CH_2CH_2$-NH_2	Ncaa = 6-aminocaproic acid
AllylOOC-$CH_2CH_2CH_2$-NH_2	Nbua = 4-aminobutyric acid
AlocHN-$CH_2CH_2CH_2CH_2CH_2CH_2$-NH_2	Namh = 1,6-diaminohexane
BocHN-$CH_2CH_2CH_2CH_2CH_2CH_2$-NH_2	
AlocHN-$CH_2CH_2CH_2CH_2$-NH_2	Namb = 1,4-diaminobutane
BocHN-$CH_2CH_2CH_2CH_2$-NH_2	
*t*BuOOC-CH_2-NH_2	Nasp = glycine
(*R*)-Ph-$CH(CH_3)$-NH_2	Nrpe = (*R*)-*N*-(1-phenylethyl)glycine

peptoids with either the possibility for charge–charge interactions *via* the side chains (**13–17**) or a covalent linkage (**18–22**). The peptoids were synthesized *via* the solid-phase submonomer approach, developed by Zuckermann *et al.*[4] Due to ease of automation we performed the peptoid synthesis at room temperature in an automated synthesizer, with coupling times of 1 hour for the acylation and 1.5 hours for the amination (Scheme 2).

We envisaged performing the synthesis of both the linear and the cyclic peptoids completely on solid support. This approach would include a side chain to side chain cyclization on solid support and therefore required appropriate orthogonally protected building blocks. The allyl ester for acid functionalities and allyloxycarbonyl carbamate (Aloc) for amine functionalities have been widely applied in classical peptide synthesis as protecting groups orthogonal to the Fmoc/Boc strategy.[19] Similarly, we selected these noble metal labile protecting groups to protect those side chain functionalities in the peptoid, envisaged for the on-bead cyclization. Other reactive side chain functionalities in the peptoids, when present, were protected with appropriate acid labile protecting groups. The precursor submonomer units mono-Boc diamines and mono-Aloc diamines were prepared from the free diamines *via* reaction with allyl-phenyl carbonate or *tert*-butoxy-phenyl carbonate respectively, following a procedure described before.[20] Amino acid allyl esters were prepared as their tosylate salts by treating the corresponding free amino acid with allyl alcohol in the presence of *p*-toluenesulfonic acid.[21] An overview of the amino building blocks used in the synthesis of peptoids **1–22** and the names of the side-chains when incorporated in the peptoid are given in Table 1.

The linear sequences of the peptoids were assembled on resin *via* the reported methodology.[4] After assembly the *N*-terminus of the peptoid was acetylated to avoid undesired side-reactions during the subsequent on-bead side-chain to side-chain cyclization. The allyl and Aloc protecting groups were subsequently selectively removed with $Pd(PPh_3)_4$ in a degassed solution of piperidine–NMP (80 : 20). At this point, the peptoid-functionalized resin was divided into two batches, to generate both the linear and the cyclic peptoids. The on-bead cyclization proved to be most efficient when HATU was used as dehydrating reagent. The use of PyBOP resulted in inferior results for this lactamization, as did the application of additional microwave radiation. Cleavage of the peptoid from the resin and purification *via* preparative RP-HPLC led to the linear and cyclic constrained peptoids in good yields with purities over 97%. Purities and molecular integrity of the HPLC-purified products were confirmed by analytical LC-ESI-MS (Experimental section).

Structural evaluation in organic solvent

The relative degree of helicity of peptoids with α-chiral aromatic side chains can be assessed by circular dichroism (CD).[22] Previous molecular modeling, NMR and X-ray crystallography studies showed that it is possible to correlate the helical secondary structure of this class of peptoids with three characteristic bands in the CD spectra at 192 nm and 202 nm for the π–π* transition and at 218 nm for the n–π* transition.[11,23] It has been shown that the CD-band intensity at 202 nm varies inversely with the helical propensity, with higher maxima indicating higher populations of *trans*-amide bond structures and thus less helical character. The intensities of the bands at 192 and 218 nm are positive indications of ordered helical folds. The ratio of the bands at 218 and 202 nm was therefore used to compare the helical propensities of all peptoids in a semi-quantitative manner. The CD maximum at 218 nm (θ_{218}) is directly proportional to the helical content and the CD band observed at 202 nm (θ_{202}) is inversely proportional to the helicity. As such the ratio $\theta_{218}/\theta_{202}$ should increase with the stability of the helical secondary structure of the peptoid. By applying this ratio, peptoids with different proportions of UV-active residues in their sequences can be compared.

Evaluation of peptoid series 1 with CD spectroscopy revealed that the linear peptoids **1–3** featured CD spectra with $\theta_{218}/\theta_{202}$ ratios that are significantly lower than that of the reference peptoid $(Nrpe)_6$ (1.25). (Fig. 1 and 2) Especially peptoid **3** features a CD spectrum with a shape and $\theta_{218}/\theta_{202}$ ratio (0.66) that is not representative of a helical conformation. These results show that replacement of two of the six Nrpe functionalities by two charged residues significantly lowers the helical stability of the peptoid. The CD spectra of the cyclic peptoids **4–6** on the other hand feature a characteristic deep minimum at 192 nm and high maximum at 218 nm, typical of the helical conformation of peptoids. (Fig. 1) The $\theta_{218}/\theta_{202}$ ratio for these peptoids has even increased with respect to $(Nrpe)_6$. Especially peptoid **6**, the cyclic counterpart of

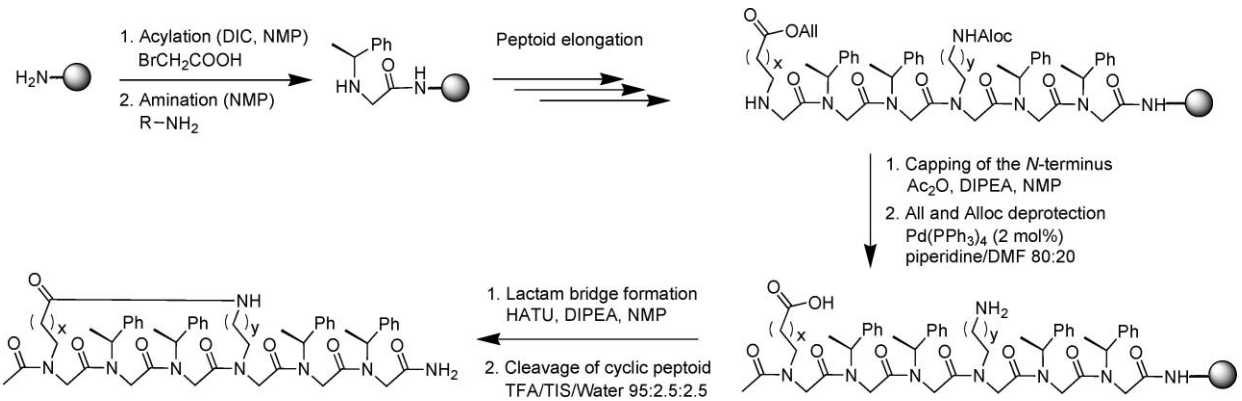

Scheme 2 General synthetic approach to linear and cyclic peptoids **1–22** *via* the submonomer approach. The assembly of the peptoid is followed by an orthogonal deprotection of the amino and the carboxylic functional groups involved in the constraining element and either direct cleavage to generate the linear peptoids or on-bead cyclization and subsequent cleavage to generate the cyclic peptoids.

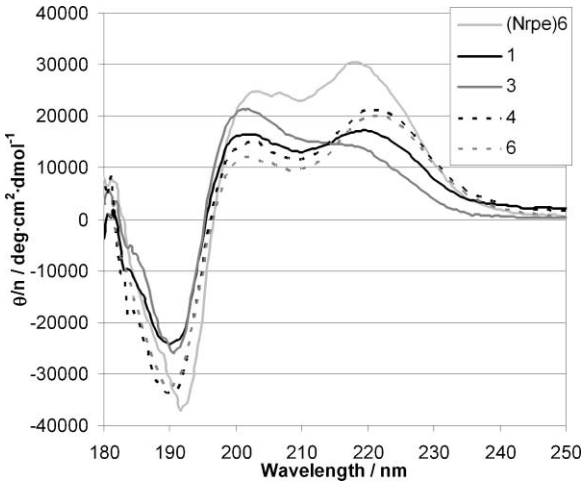

Fig. 1 Representative CD spectra of linear and cyclic peptoids of series 1 in comparison to the reference peptoid $(Nrpe)_6$ in acetonitrile. The cyclic peptoids (**4** and **6**) and reference $(Nrpe)_6$ show CD signatures typical for helical peptoids. The CD spectra of linear peptoids (**1** and **3**) feature relatively higher maxima at 202 nm, indicative of lower helical propensity.

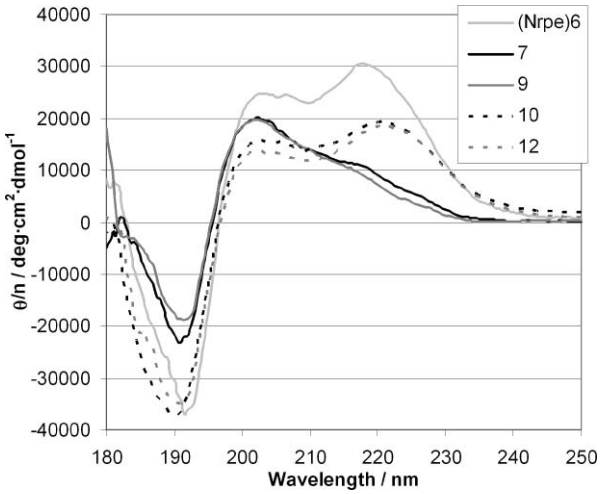

Fig. 2 Representative CD spectra of linear and cyclic peptoids of series 2 in comparison to the reference peptoid $(Nrpe)_6$ in acetonitrile. The cyclic peptoids (**10** and **12**) and reference $(Nrpe)_6$ show CD signatures typical for helical peptoids. The CD spectra of linear peptoids (**7** and **9**) are characteristic of the absence of helicity.

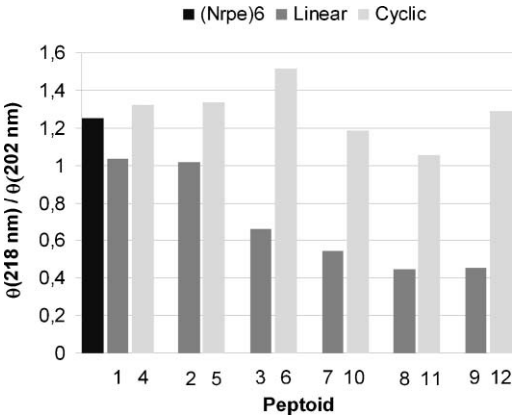

Fig. 3 Overview of $\theta_{218}/\theta_{202}$ ratios in acetonitrile for the linear and cyclic peptoids of series 1 and 2 and reference peptoid $(Nrpe)_6$.

Table 2 Per-residue molar ellipticity values (deg cm^2 dmol^{-1}) of all peptoids and reference peptoid $(Nrpe)_6$ in acetonitrile and water. n.d. = not determined

Name	θ/n (218 nm) (acetonitrile)	θ/n (202 nm) (acetonitrile)	$\theta_{218}/\theta_{202}$ (acetonitrile)	$\theta_{218}/\theta_{202}$ (water)
$(Nrpe)_6$	30484	24348	1.25	n.d.
1	16966	16357	1.04	n.d.
2	15282	14984	1.02	n.d.
3	14209	21440	0.66	n.d.
4	19881	15033	1.32	n.d.
5	19342	14482	1.34	n.d.
6	18509	12224	1.51	n.d.
7	10784	19896	0.54	n.d.
8	8861	19786	0.45	n.d.
9	8964	19637	0.46	n.d.
10	18657	15745	1.18	n.d.
11	17802	16809	1.06	n.d.
12	17481	13591	1.29	n.d.
13	6585	11248	0.59	n.d.
14	3275	4821	0.68	n.d.
15	8943	17721	0.50	n.d.
16	5466	7136	0.77	n.d.
17	14009	17490	0.80	n.d.
18	14916	12789	1.17	n.d.
19	14957	13826	1.08	0.78
20	20074	16240	1.24	0.78
21	20011	13325	1.50	0.85
22	14813	10551	1.40	0.63

peptoid **3**, features a high $\theta_{218}/\theta_{202}$ ratio (1.51). The introduction of a covalent bridge between the side-chains at positions *i* and *i* + 3 at the *N*-terminus of the peptoid thus in all cases stabilizes the helical conformation of the peptoid. The length of the lactam bridge, as varied between peptoid **4–6**, seems to play a fine-tuning role in determining the extent of the helical character.

The peptoids in series 2 have the constraining element positioned at the *C*-terminus of the peptoid. The linear peptoids **7–9** featured CD spectra that are characteristic of the absence of helicity. (Fig. 2) The $\theta_{218}/\theta_{202}$ ratios are all in the regime of 0.5, independent of side chain length (Fig. 3,Table 2). This shows that the insertion of two charged side chains at the *C*-terminus of the linear peptoids results in complete destabilization of the helical conformation. The effect is significantly stronger in comparison with the placement of the charged side chains at the *N*-terminus of the peptoids, as for peptoids **1–3** in series 1. The incorporation of a lactam bridge in peptoids **10–12** results however again in CD spectra typical for peptoids with a high helical character. The length of the side-chains forming the lactam bridge again has a slight differentiating effect on the stability. The results on series 2 clearly show that the cyclization of two side-chains in the peptoids has a strong helix stabilizing effect; without this cyclization the peptoids lose their helicity completely. The importance of a helix stabilizing element at the *C*-terminus of peptoids has been previously described.[11] Typically this has been an aromatic α-chiral substituent. The results on series 2 show that a covalent bridge from the *C*-terminus to peptoid residue *i* + 3 can also fulfil this stabilizing role. When the cyclic bridge is absent and only a linear amine is positioned at the *C*-terminus, the peptoid completely loses helical character. The helical structure in

series 2 is thus maintained mainly due to the constraining linkage introduced in the *C*-terminus.

The strong stabilizing effect of the covalent bridge at the *C*-terminus of the series 2 peptoids on the helical character prompted us to investigate the possibility to replace more Nrpe monomer units by achiral, linear, and polar monomers. Such a library would allow us to investigate the reduction of Nrpe monomers and the generation of short water-soluble peptoids, possibly with helical character. Based on the stabilizing element found in series 2, series 3 was designed with the side chain to side chain covalent bridge located at positions 3 and 6. For a systematic analysis of the influence of the replacement of Nrpe units and to ensure water-solubility, an acidic achiral side chain was introduced in the monomer sequence scanning every available position (1, 2, 3, and 5). This design resulted in peptoids **18–21**. Additionally, peptoid **22** was designed featuring two achiral side chains, bringing down the total content of aromatic α-chiral substituents to only 33%. For comparison linear analogs **13–17** were made.

Analysis of the CD spectra of peptoids **13–22** in acetonitrile (Fig. 4 and 5, Table 2) revealed that the cyclic peptoids **18–22** again featured CD signatures indicative of a high helical content of the peptoid. The CD spectra and the $\theta_{218}/\theta_{202}$ ratios are very similar to constrained peptoid **11**, featuring 4 Nrpe groups, but without an additional water-solubilizing group. Even peptoid **22**, featuring only 2 aromatic α-chiral substituents, has a high helical character in acetonitrile. The linear analogs **13–17** feature, as expected, a CD spectrum indicative of the absence of a helical conformation. The cyclic element at the *C*-terminus is thus capable of stabilizing the helical conformation of a peptoid featuring as little as 33% Nrpe elements. This results in helical peptoids that do not follow the previously formulated design rules that *N*-α-stereocenters and aromatic substituents should be present in at least 50% of the monomer composition, and that the last residue (at the *C*-terminus) should feature an α-chiral substituent. The capability of the cyclization to induce helicity in such short and diversely substituted peptoids, shows the strength of the cyclization approach.

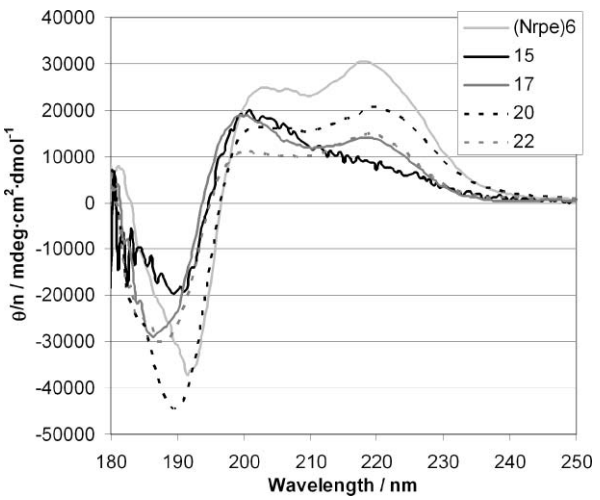

Fig. 4 Representative CD spectra of linear and cyclic peptoids of series 3 in acetonitrile. The cyclic peptoids (**20** and **22**) show CD signatures typical for helical peptoids. The CD spectra of linear peptoids (**15** and **17**) are characteristic of the absence of helicity.

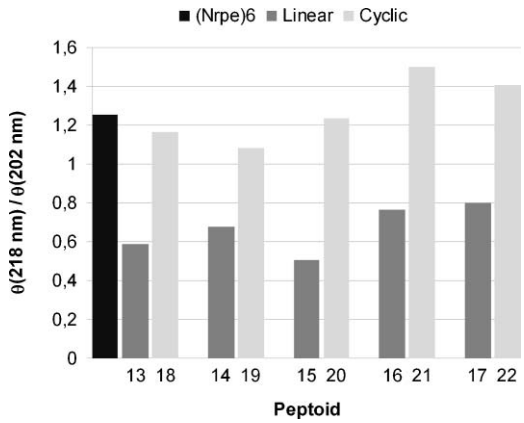

Fig. 5 Overview of $\theta_{218}/\theta_{202}$ ratios in acetonitrile for the linear and cyclic peptoids of series 2 and reference peptoid $(Nrpe)_6$.

Structural evaluation in water

Encouraged by the strong stabilization of helical peptoids **18–22** in acetonitrile, we evaluated the folding of the peptoids of series 3 in aqueous media (Fig. 6 and 7, Table 2). Due to the incorporation of the acidic side chains, these peptoids featured good water solubility. The CD spectra of the peptoids of series 3 in buffered (pH 7.2) water (Fig. 6) featured a moderate decrease in the $\theta_{218}/\theta_{202}$ ratio in comparison with the CD spectra of these peptoids in acetonitrile. Nevertheless, the signature of the curve still reflects the presence of a helical conformation. The peptoids featuring 50% Nrpe monomers (**19–21**) feature a higher $\theta_{218}/\theta_{202}$ ratio (~0.80) than the peptoid that features only 33% Nrpe monomers (**22**, $\theta_{218}/\theta_{202}$ ratio 0.62), showing that especially in water structuring steric side chain interactions still play a major role. It should be noted that, in contrast to the longer helical peptoid in water reported in literature,[12–14] the cyclic peptoids reported here do not feature α-chiral hydrophilic side chains, but simple linear side chains. Overall the results show that water in general has less helix promoting character for peptoids than acetonitrile does. The

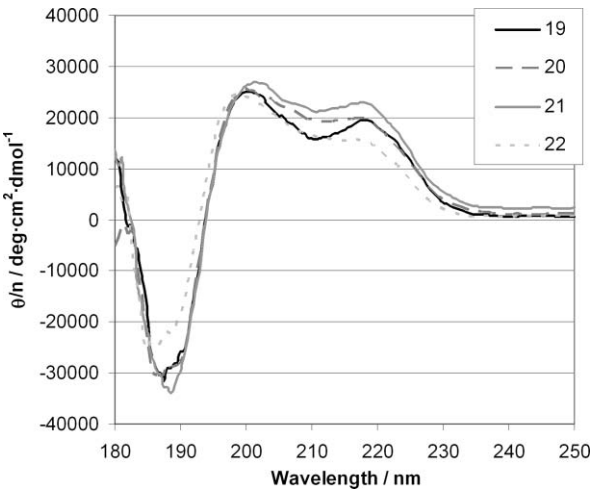

Fig. 6 CD spectra of cyclic peptoids **19–22**, in water at pH 7.2. The effect of the constraining lactam bridge on the helical propensity is reflected in the typical CD signature of helical peptoids as observed both in acetonitrile and buffer. In aqueous media, the helical component of the peptoid is lowered compared to acetonitrile.

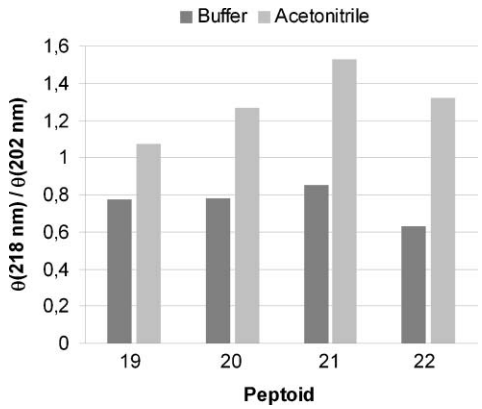

Fig. 7 Overview of $\theta_{218}/\theta_{202}$ ratios in buffer (pH 7.2) and acetonitrile for the cyclic peptoids **19–22** of series 3.

short peptoids stabilized *via* a covalent bridge at the *C*-terminus presented here, however retain significant helical character when 50% Nrpe monomers act in cooperativity with the cyclization element.

Conclusions

We have developed a novel approach for the stabilization of short helical peptoids in both organic and aqueous media. The introduction of a covalent constraining element linking two consecutive turns of the helix, resulted in the induction of a helical secondary structure in peptoids that did not feature such a stable secondary structure without this constraining element. The strategy is highly effective in organic media, resulting in helical peptoids when featuring only 33% aromatic α-chiral substituents and lacking an aromatic α-chiral substituent on the *C*-terminus. The cyclization of the peptoids, also results in the stabilization of the helical conformation in water, preferably in the presence of 50% aromatic α-chiral substituents. The cyclization strategy for peptoids thus offers a fruitful entry to generate (short) helical peptoids, folding in both organic and in aqueous solution. The approach avoids the need to introduce high percentages of aromatic α-chiral substituents, enabling both higher substituent diversity and water solubility. This opens the way to generate diversely substituted helical peptoids for biological applications.

Experimental

Peptoid synthesis

Peptoids were synthesized on a 68 μmol scale (200 mg of resin) using the submonomer approach in an automated synthesizer. One cycle of peptoid elongation consisted of the following steps. The Rink amide MBHA resin was first swollen with *N*-methyl-2-pyrrolidone (NMP) (1 × 15 min) for initial resin swelling and the Fmoc protecting group was removed by treatment with 20% piperidine–NMP (3 mL, 1 × 20 min), then washed with NMP (5 × 30 s). The deprotected resin was treated for 30 min. with a mixture containing bromoacetic acid (30 equiv. 2 M solution in NMP), diisopropylcarbodiimide (DIC, 30 equiv. 2 M solution in NMP) followed by an intensive washing step with NMP (8 × 60 s). Amination was performed consecutively adding the appropriate primary amine (35 equiv. 1 M solution in NMP) and reacting for 90 min. Then, the resin was washed with NMP (8 × 60 s). These steps were repeated until the peptoid sequence was complete. Capping of the *N*-terminus was performed by treatment with acetic anhydride (20 equiv.), DIEA (5 equiv.) and HOBt (0.6 equiv.) in NMP (5 mL, 1 × 15 min) and the capped resin was washed with NMP (5 × 60 s).

The allyl and Aloc protecting groups were removed in the presence of a catalytic amount of $Pd(PPh_3)_4$. First, the resin was washed with NMP (5 × 30 s), CH_2Cl_2 (5 × 30 s), Et_2O (5 × 30 s) and dried under vacuum for 3 h. Then, a degassed solution of piperidine–DMF solution (80:20) was prepared while argon was bubbled through the mixture and $Pd(PPh_3)_4$ (0.2 equiv) was added. The resin was then swollen with this degassed mixture and the reaction was shaken overnight under argon. Finally, the resin was washed with NMP (3 × 2 min), a 0.02 M solution of Et_2NCS_2Na in NMP (3 × 2 min), again with NMP (5 × 1 min), CH_2Cl_2 (5 × 2 min) and finally Et_2O (5 × 2 min).

Linear peptoids. The resin was washed with NMP (5 × 30 s), CH_2Cl_2 (5 × 30 s) and Et_2O (5 × 30 s) and dried under vacuum for 3 h. The resin was treated for 15–20 min with a cleavage cocktail composed of 2.5% v/v water and 2.5% v/v triisopropylsilane (TIPS) in trifluoroacetic acid (TFA). The cleaved resin was washed with TFA (2 × 15 s) and the cleaved peptoid was collected, concentrated by rotary evaporation into less than 1 mL solution and redissolved in H_2O–MeCN and lyophilized to dryness.

Cyclic peptoids. To the Aloc/Allyl deprotected peptoid resin was added HATU (3 equiv) and DIEA (9 equiv) in NMP and shaken 24 h to undergo cyclization. After washing the resin with NMP (5 × 30 s), the peptoid was cleaved from the resin as described for the linear peptoids. The crude obtained was dissolved in H_2O–MeCN and lyophilized to dryness.

The crude reaction mixture of each peptoid synthesized was analyzed by LC-MS. Peptoids were then purified by reverse-phase HPLC on a Nucleodur C18 Gravity column (125 × 21 mm, Macherey-Nagel) with a linear gradient of A (0.1% HCOOH in H_2O) and B (0.1% HCOOH in MeCN) from 20% of B to 40% of B and flow rate of 25 mL min^{-1} and were detected at 210 nm, 254 nm and 280 nm using a diode array UV/VIS detector. The identities and purities of the purified peptoids were assessed by LC-ESI-MS (Table 3). Following purification, all peptoids were lyophilized and kept at −20 °C.

Circular dichroism spectroscopy

CD spectra were recorded on a JASCO-715 spectrometer at room temperature in acetonitrile or in a 5 mM sodium phosphate buffer (pH 7.2) using a 0.1 cm path length CD cell. Each peptoid was analyzed at a concentration of 20–60 μM. The final concentration of the peptoid solutions was determined immediately before obtaining the CD spectrum by the UV absorbance at 210 nm. Spectra represent the average of 20 scans (0.5 nm data pitch, continuous scanning mode, 20 nm min^{-1} scanning speed, 0.5 nm bandwidth) and were smoothed by Jasco software. Data were converted to mean-residue ellipticity MRE (in deg cm^2 $dmol^{-1}$ $residue^{-1}$) according to the equation:

$$\mathrm{MRE} = \mathrm{CD\ effect}/Cln_{\mathrm{res}}$$

Here the CD effect is in millidegrees, the concentration (C) is in moles per litre, the path length (l) is in millimetres and n_{res} is the number of residues.

Table 3 Overview of synthesized linear and cyclic peptoids **1–22**, observed molecular mass and synthetic yields. All peptoids featured >97% purity

Peptoid	Calculated mass $[M + H]^+$	Observed mass $[M + H^+]^+$	Yield (%)
1	975.5	975.4	44
2	1003.6	1003.5	34
3	1031.6	1031.6	34
4	957.5	957.3	14
5	985.6	985.3	7
6	1013.6	1013.3	6
7	975.5	975.4	11
8	1003.6	1003.4	23
9	1031.6	1031.5	19
10	957.5	957.1	9
11	985.6	985.1	5
12	1013.6	1013.1	5
13	957.5	957.5	12
14	957.5	957.5	13
15	957.5	957.4	24
16	957.5	957.4	2
17	911.4	911.4	2
18	939.5	939.3	5
19	939.5	939.1	9
20	939.5	939.2	7
21	939.5	939.2	11
22	893.4	893.1	11

The ratio of the bands at 218 and 202 nm was used to compare the helical propensities of all peptoids in a semi-quantitative manner.

Acknowledgements

This work was supported by a Sofja Kovalevskaja Award of the Alexander von Humboldt Foundation and the BMBF to L.B., and the Spanish Ministerio de Educación y Ciencia with a Postdoctoral Fellowship to B.V.

Notes and references

1 (*a*) S. H. Gellman, *Acc. Chem. Res.*, 1998, **31**, 173–180; (*b*) K. Kirshenbaum, R. N. Zuckermann and K. A. Dill, *Curr. Opin. Struct. Biol.*, 1999, **9**, 530–535; (*c*) D. J. Hill, M. J. Mio, R. B. Prince, T. S. Hughes and J. S. Moore, *Chem. Rev.*, 2001, **102**, 3892–4011.

2 (*a*) R. P. Cheng, S. H. Gellman and W. F. DeGrado, *Chem. Rev.*, 2001, **101**, 3219–3232; (*b*) D. Seebach, D. F. Hook and A. Glattli, *Biopolymers*, 2006, **84**, 23–37; (*c*) C. M. Goodman, S. Choi, S. Shandler and W. F. DeGrado, *Nat. Chem. Biol.*, 2007, **3**, 252–262; (*d*) A. D. Bautista, C. J. Craig, E. A. Harker and A. Schepartz, *Curr. Opin. Chem. Biol.*, 2007, **11**, 685–692.

3 R. J. Simon, R. S. Kania, R. N. Zuckermann, V. D. Huebner, D. A. Jewell, A. Banville, S. Ng, L. Wang, S. Rosenberg, C. K. Marlowe, D. C. Spellmeyer, R. Tan, A. D. Frankel, D. V. Santi, F. E. Cohen and P. A. Bartlett, *Proc. Natl. Acad. Sci. U. S. A.*, 1992, **89**, 9367–9371.

4 R. N. Zuckermann, J. M. Kerr, S. B. H. Kent and W. H. Moos, *J. Am. Chem. Soc.*, 1992, **114**, 10646–10647.

5 S. M. Miller, R. J. Simon, S. Ng, R. N. Zuckermann, J. M. Kerr and W. H. Moos, *Bioorg. Med. Chem. Lett.*, 1994, **4**, 2657–2662.

6 (*a*) J. A. Gibbons, A. A. Hancock, C. R. Vitt, S. Knepper, S. A. Buckner, M. E. Burne, I. Milicic, J. F. Kerwin, L. S. Richter, E. W. Taylor, K. L. Spear, R. N. Zuckermann, D. C. Spellmeyer, R. A. Braeckman and W. H. Moos, *J. Pharmacol. Exp. Ther.*, 1996, **277**, 885–899; (*b*) A. E. Barron and R. N. Zuckermann, *Curr. Opin. Chem. Biol.*, 1999, **3**, 681–687; (*c*) J. A. Patch and A. E. Barron, *Curr. Opin. Chem. Biol.*, 2002, **6**, 872–877; (*d*) J. A. Patch and A. E. Barron, *J. Am. Chem. Soc.*, 2003, **125**, 12092–12093; (*e*) C. W. Wu, S. L. Seurynck, K. Y. C. Lee and A. E. Barron, *Chem. Biol.*, 2003, **10**, 1057–1063; (*f*) T. Hara, S. R. Durell, M. C. Myers and D. H. Appella, *J. Am. Chem. Soc.*, 2006, **128**, 1995–2004; (*g*) R. C. Elgersma, G. E. Mulder, J. A. W. Kruijtzer, G. Posthuma, D. T. S. Rijkers and R. M. J. Liskamp, *Bioorg. Med. Chem. Lett.*, 2007, **17**, 1837–1842.

7 D. Seebach, A. K. Beck and D. J. Bierbaum, *Chem. Biodiversity*, 2004, **1**, 1111–1239.

8 (*a*) K. Kirshenbaum, A. E. Barron, R. A. Goldsmith, P. Armand, E. K. Bradley, K. T. V. Truong, K. A. Dill, F. E. Cohen and R. N. Zuckermann, *Proc. Natl. Acad. Sci. U. S. A.*, 1998, **95**, 4303–4308; (*b*) A. T. Fafarman, P. P. Borbat, J. H. Freed and K. Kirshenbaum, *Chem. Commun.*, 2007, **4**, 377–379.

9 C. W. Wu, T. J. Sanborn, R. N. Zuckermann and A. E. Barron, *J. Am. Chem. Soc.*, 2001, **123**, 2958–2963.

10 P. Armand, K. Kirshenbaum, R. A. Goldsmith, S. Farr-Jones, A. E. Barron, K. T. V. Truong, K. A. Dill, D. F. Mierke, F. E. Cohen, R. N. Zuckermann and E. K. Bradley, *Proc. Natl. Acad. Sci. U. S. A.*, 1998, **95**, 4309–4314.

11 C. W. Wu, T. J. Sanborn, K. Huang, R. N. Zuckermann and A. E. Barron, *J. Am. Chem. Soc.*, 2001, **123**, 6778–6784.

12 T. J. Sanborn, C. W. Wu, R. N. Zuckermann and A. E. Barron, *Biopolymers*, 2002, **63**, 12–20.

13 S. B. Y. Shin and K. Kirshenbaum, *Org. Lett.*, 2007, **9**, 5003–5006.

14 T. S. Burkoth, E. Beausoleil, S. Kaur, D. Tang, F. E. Cohen and R. N. Zuckermann, *Chem. Biol.*, 2002, **9**, 647–654.

15 (*a*) M. Chorev, E. Roubini, R. L. McKee, S. W. Gibbons, E. Goldman, M. P. Caulfield and M. Rosenblatt, *Biochemistry*, 1991, **30**, 5968–5974; (*b*) D. Y. Jackson, D. S. King, J. Chmielewski, S. Singh and P. G. Schultz, *J. Am. Chem. Soc.*, 1991, **113**, 9391–9392; (*c*) H. E. Blackwell and R. H. Grubbs, *Angew. Chem., Int. Ed.*, 1998, **37**, 3281–3284; (*d*) L. D. Walensky, A. L. Kung, I. Escher, T. J. Malia, S. Barbuto, R. D. Wright, G. Wagner, G. L. Verdine and S. J. Korsmeyer, *Science*, 2004, **305**, 1466–1470; (*e*) G. Dimartino, D. Y. Wang, R. N. Chapman and P. S. Arora, *Org. Lett.*, 2005, **7**, 2389–2392; (*f*) A. K. Galande, K. S. Bramlett, J. O. Trent, T. P. Burris, J. L. Wittliff and A. F. Spatola, *ChemBioChem*, 2005, **6**, 1991–1998; (*g*) E. Vaz and L. Brunsveld, *Org. Lett.*, 2006, **8**, 4199–4202.

16 (*a*) G. Bitan, I. Sukhotinsky, Y. Mashriki, M. Hanani, Z. Selinger and C. Gilon, *J. Pept. Res.*, 1997, **49**, 421–426; (*b*) D. Besser, B. Muller, P. Kleinwachter, G. Greiner, L. Seyfarth, T. Steinmetzer, O. Arad and S. Reissmann, *J. Prakt. Chem.*, 2000, **342**, 537–545; (*c*) A. Friedler, D. Friedler, N. W. Luedtke, Y. Tor, A. Loyter and C. Gilon, *J. Biol. Chem.*, 2000, **275**, 23783–23789; (*d*) S. Gazal, G. Gellerman, E. Glukhov and C. Gilon, *J. Pept. Res.*, 2001, **58**, 527–539; (*e*) S. Reissmann and D. Imhof, *Curr. Med. Chem.*, 2004, **11**, 2823–2844.

17 S. B. Y. Shin, B. Yoo, L. J. Todaro and K. Kirshenbaum, *J. Am. Chem. Soc.*, 2007, **129**, 3218–3225.

18 J. M. Holub, H. Jang and K. Kirshenbaum, *Org. Lett.*, 2007, **9**, 3275–3278.

19 P. Grieco, P. M. Gitu and V. J. Hruby, *J. Pept. Res.*, 2001, **57**, 250–256.

20 M. Pittelkow, R. Lewinsky and J. B. Christensen, *Synthesis*, 2002, **15**, 2195–2202.

21 H. Waldmann and H. Kunz, *Liebigs Ann. Chem.*, 1983, **10**, 1712–1725.

22 R. W. Woody, *Methods Enzymol.*, 1995, **246**, 34–71.

23 (*a*) K. Huang, C. W. Wu, T. J. Sanborn, J. A. Patch, K. Kirshenbaum, R. N. Zuckermann, A. E. Barron and I. Radhakrishnan, *J. Am. Chem. Soc.*, 2006, **128**, 1733–1738; (*b*) C. W. Wu, K. Kirshenbaum, T. J. Sanborn, J. A. Patch, K. Huang, K. A. Dill, R. N. Zuckermann and A. E. Barron, *J. Am. Chem. Soc.*, 2003, **125**, 13525–13530.

